JOURNAL OF CATALYSIS 157, 66–75 (1995)

Control of Intrazeolitic Gallium Cation Content and Its Effects on C_2 Dehydrogenation in Ga-MFI Catalysts

Kerry M. Dooley,[1] Trent F. Guidry, and Geoffrey L. Price

Department of Chemical Engineering, Louisiana State University, Baton Rouge, Louisiana 70803

Received December 16, 1994; revised June 6, 1995; accepted July 26, 1995

Ga-doped MFI zeolites are selective C_2 and higher alkane dehydrogenation catalysts. The balance between zeolite proton sites and exchanged Ga-cations, which is known to critically affect the formation of aromatics, is itself greatly affected by the extent of Ga reduction, steaming, and treatment with oxidizers. Also, although the reaction can be inhibited by H_2 and CH_4, at short times on stream the presence of CH_4 can in some cases enhance the formation of aromatics. The reaction of ethane at low alkane pressures has been used to separate these effects from site deactivation by coking. The kinetics studies were supplemented with site characterization experiments, including thermal analysis of adsorbed 1-propanamine, TPO of the carbonaceous residues, XRD, and FTIR of the catalyst and of adsorbed 1-propanamine and pyridine. These studies show that at reaction conditions small quantities of H_2O and/or O_2 can transform intrazeolite Ga-cation sites back to protons and gallium oxide. This transformation inhibits the formation of aromatics except in the case of low levels of protons, where the yield to aromatics can actually increase. The results are interpreted in terms of the dual-function mechanism for alkane dehydrogenation.

INTRODUCTION

Gallium-loaded zeolites, especially Ga-MFI (Ga-ZSM-5), are well-known alkane aromatization catalysts, studied extensively of late (1). These materials may also be useful for other chain-building and dehydrogenation reactions, for example the transalkylation of aliphatic amines (2).

In a series of publications, we have reported that reduction of impregnated or mechanically mixed Ga_2O_3/H-MFI catalysts with H_2 or hydrocarbons is an effective method for incorporation of Ga^+ into the cationic positions of the zeolite framework (3–8). In the present investigation we have also used H_2 reduction of Ga-MFI to replace protons in the parent H-MFI with Ga^+ ions. We and others have also studied the relationship between activity and structure for Ga_2O_3/H-MFI propane aromatization catalysts. It was found that reduction with H_2 is the most beneficial pretreatment, again giving Ga^+ cations within the zeolite prior to reaction (3, 4, 8–11). We found a good correlation between increasing activity and yield to aromatics and increasing replacement of protons by Ga^+, up to a high degree of replacement (3, 8). The reduction of Ga_2O_3 appeared to be kinetically limited by the number of available cation sites in the host zeolite (4, 5). These conclusions have been challenged by results on initial yields to aromatics suggesting that the alkane is activated by a separate Ga_2O_3 phase (12). They have also been challenged by a series of propane dehydrogenation experiments which showed maximum initial conversion and selectivity to aromatics for Ga/(Ga + H) ratios of ~0.4 (13). These experiments suggest that a true bifunctional mechanism is operative, with both proton and Ga-cation sites involved in the transformation of every reactant molecule to a dehydrogenated product. It was hypothesized that the Ga^+ or $[GaO]^+$ cations might abstract a hydride ion to effect the initial carbenium ion formation, while protons were used to regenerate these Lewis sites.

We and others have subsequently observed that oxidation with O_2 after the initial reduction can produce a more active catalyst for alkane aromatization (9–11). In *n*-butane aromatization, a notable increase in the aromatics selectivity was observed with an H-MFI catalyst when 5 mol% O_2 was added to the feed (14). The promotional effect of O_2 on aromatics selectivity was attributed to the faster removal of surface hydrogens from active sites as water. This effect of O_2 was again observed in pulse studies of butane dehydrogenation catalyzed by Ga-Zn-MFI, using O_2 supplied from a mixed metal oxide (15). CO and CO_2 have been found to have similar promotional effects with similar catalysts (16).

Therefore we wish to clarify the effects of various catalyst pretreatments and the presence of certain gases during reaction on the behavior of Ga-loaded MFI. We show that these effects arise primarily from changes in the balance between intrazeolitic Ga cations (at exchange sites) and protons. Such a study sheds further light on the bifunctional nature of alkane dehydrogenations in these catalysts. Be-

[1] To whom correspondence should be addressed.

0021-9517/95 $12.00

cause we have found that ethane aromatization appears to be more sensitive to these effects, we have used this reaction for catalyst characterization. Some of the effects we study here are also applicable to the activation of CH_4 by Ga-MFI, which is important in the application of similar catalysts to NO_x reduction with CH_4 (17).

METHODS

Catalyst Preparation and Characterization

UOP MFI zeolite with a SiO_2/Al_2O_3 mole ratio of 40 was used as the catalyst base material in a fully protonated form which we refer to as H-MFI. A Ga-impregnated catalyst (denoted Ga_2O_3/MFI-i prior to reduction, Ga-MFI-i after reduction) was prepared by incipient wetness (2). The Ga loading was 7.1 g Ga_2O_3/100 g dry zeolite, or 0.95 Ga atom/framework Al. A physically mixed material (Ga_2O_3/MFI-m prior to reduction, Ga-MFI-m after reduction), also with close to 1 Ga/Al, was prepared by ball-milling the oxide and zeolite for 3 h. All catalysts were pelletized, then ground and sieved to 0.18–0.42 mm (20–40 mesh) prior to utilization.

The Ga_2O_3/MFI-i catalysts were typically reduced in flowing 30% H_2/70% He mixture using a 1 K/min rise to 848 K, then holding for 3 h (TGA or FTIR experiments) or 6 h (microreactor experiments). The longer times in the microreactor were necessary because the sample sizes were larger. The Ga_2O_3/MFI-m catalysts required even longer holding times for complete reduction, up to 18 h in the microreactor at 848 K. Reoxidation was for 2 h at 823 K in flowing 30% O_2/He, except where noted.

Reported surface areas are by the BET method with an Omicron Omnisorb-360 analyzer. X-ray powder diffraction patterns were obtained using a Scintag PAD-V Powder X-Ray Diffractometer using Cu $K\alpha$ radiation. The scan range was 20–50° (2θ) at 0.02°/s. These spectra were compared to a standard computed powder pattern for MFI zeolite (18).

A Perkin–Elmer TGA7 microbalance was used to detect weight change upon thermal treatment of the catalysts in He or a mixture of He with a reagent gas. Ten to fifteen milligrams of sample was weighed out in the platinum microbalance pan. The following sequence of treatments was typically performed:

1. Drying in He (100 cm^3/min) by programming from 298 to 848 K at 10 K/min with a final hold of 10 min.
2. Isothermal reduction at the desired temperature using 50 cm^3 of a 1:1 mixture of He/H_2 plus 50 cm^3 of He which purged the balance mechanism. After the weight stopped changing, the sample was cooled rapidly.
3. Treatment with a reacting gas mixture as described below.
4. Propanamine adsorption for 5 min at 323 K. 1-Propanamine (1-PA) was delivered by bubbling 50 cm^3/min of He through the liquid at ambient temperature, then it was mixed with the diluent He.
5. TGA in He by programming from 323 to 823 K at 5 K/min.

IR spectra were taken in the transmittance mode using an IBM IR-30 FTIR. The zeolites were pressed into self-supporting wafers, 6.5 mg/cm^2, which were loaded into a controlled atmosphere quartz IR cell and outgassed ($<10^{-3}$ Torr, 1 Torr = 133.3 Pa) for 2 h at 773 K or 1 h at 823 K prior to further treatment.

For pyridine adsorption experiments, the samples were pretreated as described under Results, evacuated for 15 min at 823 K, then cooled to 423 K under vacuum; reference spectra were then recorded. Then the samples were cooled to 373 K, exposed to pyridine vapor for 10 min, and heated to 423 K while evacuating for 15 min; the spectra were then recorded.

Reaction Apparatus and Procedure

The upflow tubular reactor was stainless steel, i.d. 1.0 cm and length 20 cm, containing 0.8 g catalyst on a quartz wool bed. The microreactor system, the gases used, and the product analysis were the same as in a previous study (19). All samples were purged for at least 1 h in He flow at the initial temperature prior to a reaction experiment.

Both selectivities and conversions were computed on the basis of number of moles of carbon, e.g., if C_i = mol of compound i, containing j carbon atoms, then

$$\sum C_{\text{product}} = \sum jC_i = C_{CH_4} + 2\,C_{C_2H_4} + \cdots + 6\,C_{C_6H_6} + \cdots \quad [1]$$

$$S_{C_2H_4} = 2\frac{C_{C_2H_4}}{\sum C_{\text{product}}} \times 100. \quad [2]$$

Yields were calculated as the products of selectivity and ethane conversion.

RESULTS

The BET surface areas (unreduced but dried) were unaffected by impregnation, H-MFI, 315 ± 10 m^2/g and Ga_2O_3/MFI-i, 320 ± 15 m^2/g. XRD analysis of H-MFI and unreduced Ga_2O_3/MFI-i and Ga_2O_3/MFI-m gave expected results for well-crystallized zeolite, with no effects resulting from impregnation for Ga_2O_3/MFI-i. The XRD spectra were unaffected by any combination of pretreatments with He, 30% O_2/He (823 K), or 30% H_2/He (848 K). No angular shifts were observed upon long-term reaction of ethane, although there was a slight decrease in signal-to-noise ratio. The major changes in XRD spectra took place when O_2

TABLE 1

Summary of Ethane Dehydrogenation Results for Ga/MFI-i Catalyst[a]

Pretreatment	Additive	% Conversion	% Yield, aromatics	% wt. loss in tpo
Reduced, 6 h	None	7.0	3.9	4.4
Reduced, 6 h (2 cycles)	None	7.4	5.9	3.1
Reduced, 6 h, oxidized, 2 h	None	7.6	4.5	2.4
Oxidized, 6 h	None	3.6	1.2	1.9
None	None	6.6	2.2	4.2
Reduced, 6 h	33 kPa H_2	0.07	0.0	3.8
Reduced, 6 h	8.4 kPa H_2O	0.95	0.34	2.4
Reduced, 6 h (2 cycles)	18.3 kPa CO_2	7.2	5.7	3.2
Reduced, 6 h	10.1 kPa CH_4[b]	36.6	18.4	6.9
Reduced, 6 h	None[b]	16.0	9.3	2.5

[a] T = 823 K, data taken at <15 ks time on stream (average of two determinations), P_{C_2} = 12 kPa, C_2 WHSV = 1.0 h^{-1}.

[b] Same as footnote a, but P_{C_2} = 5.4 kPa and C_2 WHSV = 0.5 h^{-1}.

or H_2O were added to the ethane feed for relatively long times. Water addition caused small shifts to lower 2θ values, while for O_2 addition these shifts were more noticeable and accompanied by further decrease in signal-to-noise ratio. These changes suggest dealumination was possible for these samples, although the magnitude of these changes is also consistent with varying degrees of Ga-cation replacement in MFI. No changes were observed in XRD spectra after O_2 or H_2O additions over short (<5 ks) time periods.

Microbalance reduction of pure Ga_2O_3/MFI-i showed that complete reduction could be expected in ~2 ks at 848 K. Reductions in the microbalance for Ga_2O_3/MFI-m showed that complete reduction required an initial pelletization, followed by reduction for >20 ks at 848 K; the microreactor time was determined by removing samples from the reactor after treatments for varying times, and then completing the reductions in the microbalance. Microbalance reduction of a fully reduced, then oxidized, material showed that oxidation restored 60–70% of the original weight, corresponding roughly to $[GaO]^+$. These results are all consistent with past studies (9, 13).

Ethane Aromatization Results

A summary of initial results under common conditions for Ga_2O_3/MFI-i and Ga-MFI-i is given in Table 1. Reduction followed by oxidation increased both the overall activity and the aromatics yield. Oxidation alone was ineffective. Addition of H_2 or water to the feed greatly inhibited the reactions. Methane, on the other hand, strongly promoted the formation of aromatics at initial conditions. As seen in Fig. 1, we found that the overall activity changed in the same direction as the aromatics yield, although not always by the same percentage. In all subsequent figures only the yield to aromatics is plotted. A reaction rate in kg mol/(kg · s) can be computed by multiplying the conversions or yields in Figs. 1–4 by 6.3×10^{-8} and those in Fig. 5 by one-half this number.

In Fig. 1 it is seen that although deactivation takes place in all catalysts, the advantage of the reduced/oxidized material over its counterparts is long-lived. The order of catalyst activities shown in Fig. 1 also held for the sample prepared by physical mixing (Fig. 2), although much longer times were necessary to reduce this material. The effects are therefore seemingly independent of mode of sample preparation. The addition of a small amount of O_2 while the catalyst was on-line also resulted in a burst of activity (Fig. 3). That such a phenomenon was tied to oxidation rather than extraneous effects is clear from Fig. 3; the addition of a relatively large amount of CO_2 had little effect. On the other hand, the addition of 8.8 kPa of water while on-stream eliminated formation of aromatics imme-

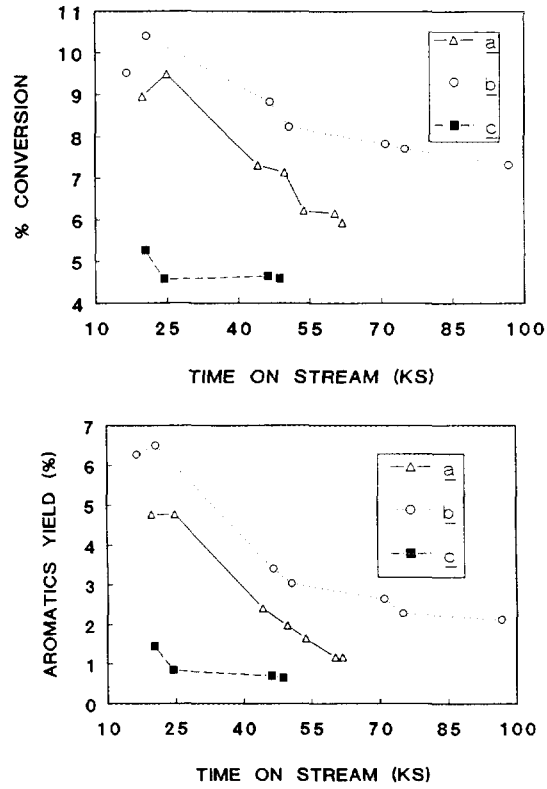

FIG. 1. Reaction of 12 kPa ethane at 843 K, WHSV = 1.0 h^{-1}, using: (a) Ga-MFI-i; (b) reoxidized Ga-MFI-i; (c) Ga_2O_3/MFI-i (no reduction), treated for 2 h at 823 K with 30% O_2/70% He.

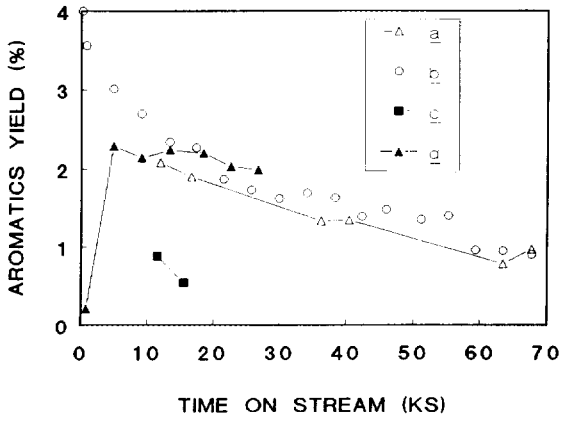

FIG. 2. Reaction of 12 kPa ethane at 823 K, WHSV = 1.0 h^{-1}, using: (a) Ga-MFI-m; (b) reoxidized Ga-MFI-m; (c) Ga_2O_3/MFI-m (no reduction), treated for 2 h at 823 K with 30% O_2/70% He; (d) Ga-MFI-m, reduced 6 h only.

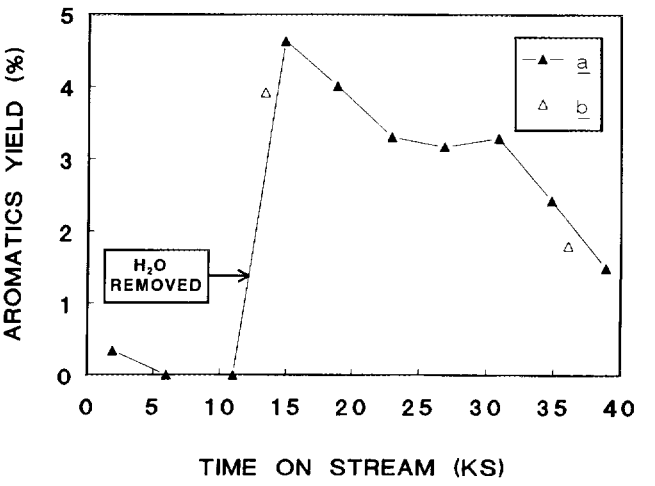

FIG. 4. Reaction of 12 kPa ethane at 823 K, WHSV = 1.0 h^{-1}, using Ga-MFI-i as follows: (a) addition of 8.4 kPa H_2O at start of reaction; (b) no added H_2O.

diately. However, this inhibition was rapidly reversible, as shown in Fig. 4.

The behavior of the catalyst in the presence of CH_4 bears closer scrutiny. Experiments with and without CH_4 are shown in Fig. 5; the promotional effect of CH_4, while short-lived, is significant. Catalysts treated with CH_4 build up large amounts of carbonaceous material (Table 1). Possibly for this reason the activity order was reversed at long times on stream, i.e., the ethane feed was usually more reactive than the ethane/methane feed (19). It was found that at similar conditions CH_4/CD_4 undergoes rapid exchange in the presence of Ga-MFI (16), but higher hydrocarbons are not formed except at higher temperatures (19). Therefore it is unlikely that the extra product at short times on stream arose from CH_4; the catalyst appears to be more active for the dehydrogenation of ethane.

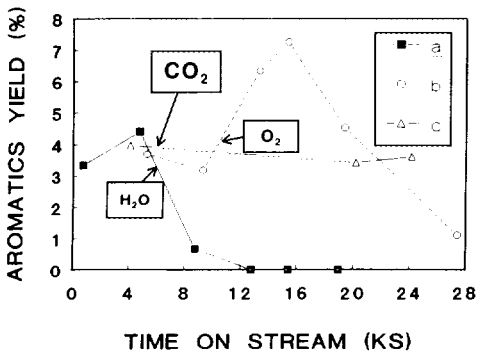

FIG. 3. Reaction of 12 kPa ethane at 823 K, WHSV = 1.0 h^{-1}, using Ga-MFI-i as follows: (a) addition of 8.8 kPa H_2O; (b) addition of 2.2 kPa O_2; (c) addition of 18 kPa CO_2. The arrows show the times the additions began.

FTIR and TGA Results

In presenting the FTIR results we compare spectra of the wafer subjected to various treatments and unreduced Ga_2O_3/MFI-i. In the spectral regions of interest, unreduced Ga_2O_3/MFI-i was similar to H-MFI, with a well-defined bridged ν_{OH} band at 3600–3610 cm^{-1}.

In Fig. 6 the effects of both H_2 reduction and slow reoxidation on the ν_{OH} region are shown. Reduction significantly attenuated the bridged hydroxyl band. Oxidation occurred upon holding the sample overnight under vacuum at r.t., followed by a temperature increase to 573 K. This treatment partly restored the band's original intensity. The

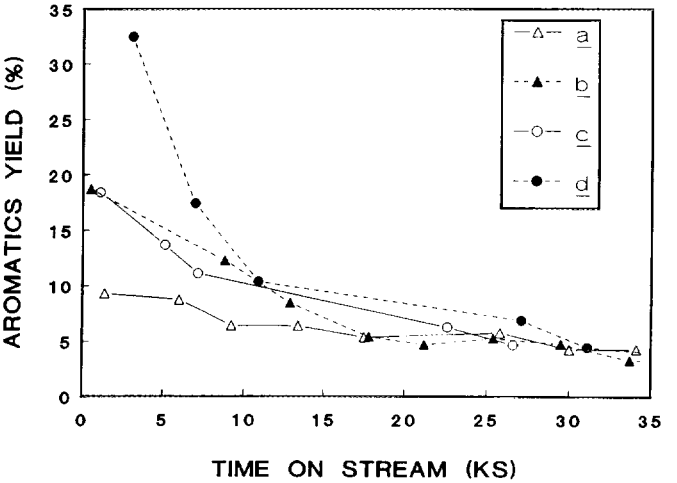

FIG. 5. Reaction of ethane (5.4 kPa, WHSV = 0.5 h^{-1}) with and without added methane (10 kPa). (a) No methane, 823 K; (b) with methane, 823 K; (c) no methane, 843 K; (d) with methane, 843 K.

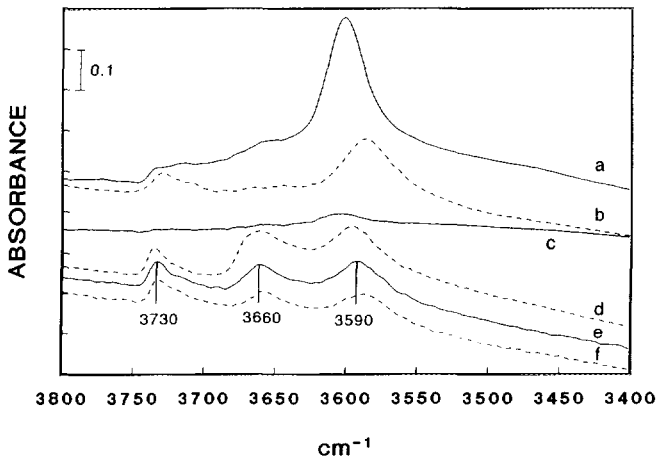

FIG. 6. FTIR spectra under vacuum (~10^{-3} Torr) of: (a) Ga_2O_3/MFI-i, dried at 773 K; (b) Ga-MFI-i, 1 h reduction at 723 K; (c) same as (b), then 2 h additional reduction at 823 K; (d) same as (c), then cooled to r.t., then heated to 573 K; (e) same as (d), then heated to 673 K; (f) same as (e), then heated to 773 K. In each case the spectra were recorded at the final temperature given.

other change upon oxidation is the appearance of a new, broad band in the 3660 cm^{-1} region. There is also an increase in intensity of the band ca. 3730 cm^{-1}. As the temperature was further increased (Fig. 6), these bands were attenuated somewhat. Such partial restoration of the bridged ν_{OH} band was also true for reoxidation using 30% O_2 at 823 K.

These results are evidence for $[GaO]^+$ (gallyl) and $[Ga(OH)_2]^+$ cations within the zeolite under oxidizing conditions. New −OH bands of steamed or air-calcined gallosilicates have been observed ca. 3660 and 3740 cm^{-1} (21–22), and in impregnated Ga_2O_3/MFI at 3660 cm^{-1} (23). These were assigned to the hydroxyl groups of extraframework Ga (24). The appearance of ν_{OH} bands associated with Ga, where none appeared prior to reduction, advances the idea that Ga is dispersed within the zeolite by being reduced.

When water is directly introduced into the IR cell the chemistry is difficult to determine, because the reaction with Ga cations is rapid. Referring to Fig. 7, we start with reduced Ga-MFI-i, where the bridged −OH band has disappeared (note that in order to highlight the differences in the spectra we have subtracted the spectrum of dried Ga_2O_3/MFI-i). However, the Brønsted sites are regenerated upon treatment at 823 K with water-saturated (at r.t.) He for 5 min. No new bands, especially those indicative of extraframework material (3660–3680 and 3740) (25–28) appear. The shifts of the restored ν_{OH} band (spectra c and d) for zeolite Brønsted sites to higher frequency (3610–3615 cm^{-1}), relative to unreduced material, is typical of association with water (20, 29). Other bands indicative of adsorbed water (3610–3615, 3625 cm^{-1}) (20) appear at 723 K, while ν_{OH} for both protonated water in H-MFI (3645–3650 and ~3710 cm^{-1}) (20) and hydrated gallium oxide in zeolites (3670 and 3740 cm^{-1}) (21–22) appear as well. These begin to merge at lower temperatures into two broad bands ca. 3720–3750 cm^{-1} and 3600–3670 cm^{-1}, as expected upon formation of H-bonded networks (29).

The attenuation of the bridged −OH band at 3600 cm^{-1} upon high temperature treatment with Ga_2O_3 has been observed previously (6, 23). But we see here that the exchange of Ga cations for protons is, at typical alkane dehydrogenation temperatures, reversible in either O_2 (Fig. 6) or H_2O (Fig. 7). One explanation for an O_2-aided recovery of proton sites would be that residual adsorbed H_2 reacts with O_2 to regenerate proton sites (Z^- represents an anionic site of the zeolite lattice,

$$[GaH_2]^+Z^- + O_2 \rightarrow [Ga(OH)_2]^+Z^- \quad [3]$$

$$H_2O + [Ga(OH)_2]^+Z^- \rightarrow Ga(OH)_3 + H^+Z^- \quad [4]$$

$$2\,Ga(OH)_3 \rightarrow Ga_2O_3 + 3\,H_2O. \quad [5]$$

Of course the −OH groups could also be recovered even in the absence of H_2, as long as traces of water were present, as follows:

$$2\,Ga^+Z^- + O_2 \rightarrow 2[GaO]^+Z^- \quad [6]$$

$$Ga^+Z^- + H_2O \rightarrow [GaO]^+Z^- + H_2 \quad [7]$$

$$H_2O + [GaO]^+Z^- \rightarrow [Ga(OH)_2]^+Z^-. \quad [8]$$

The TGA evidence favors the intermediate formation of the gallyl cations, reactions [6] and [7], especially at

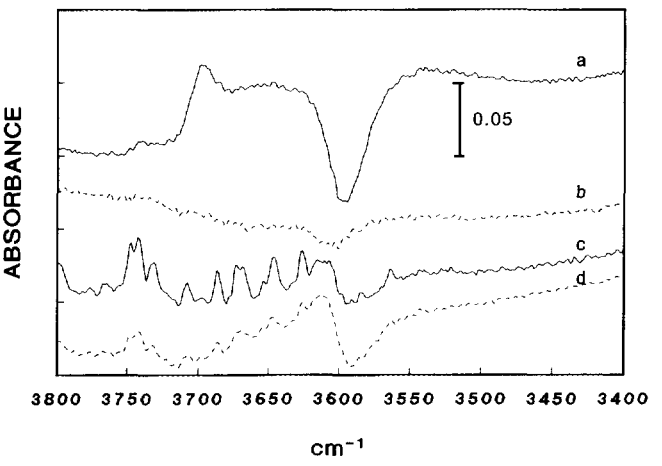

FIG. 7. FTIR difference spectra of Ga-MFI-i, referenced to dried (773 K) Ga_2O_3/MFI-i. Spectrum (a) taken immediately after reduction at 823 K. Other treatments: (b) 5 min H_2O-saturated He, at 823 K; (c) same as (b), but at 723 K; (d) same as (b), but at 623 K. Spectra were taken in each case at the final temperature given.

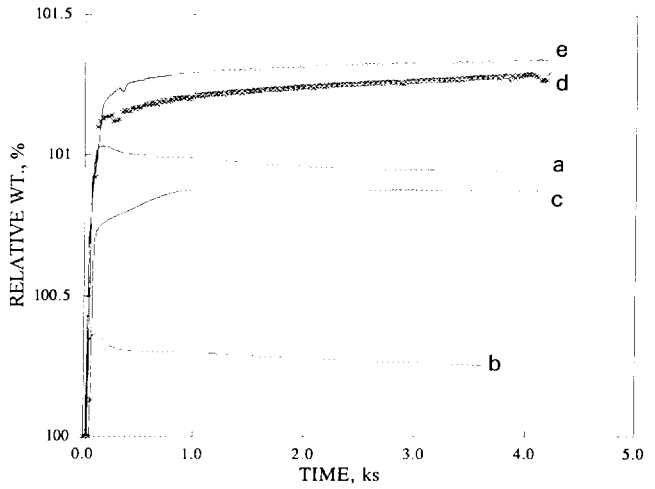

FIG. 8. Microbalance TGA at 823 K of Ga-MFI-i for reaction with: (a) H_2O-saturated He; (b) H_2O-saturated He, but after 1-PA adsorption and thermal analysis; (c) 30% O_2/70% He; (d) 12% C_2H_6/2% O_2/86% He; (e) H_2O-saturated 30% O_2/70% He.

brief times and low water partial pressures. Examining the adsorption data at 823 K shown in Fig. 8, we see that both O_2 and H_2O used separately lead to roughly the same weight increase for the reduced Ga-MFI-i. Based on the stoichiometry of reaction [6] or [7], these numbers correspond to 90% conversion to the gallyl cation for reaction with water (79% if the H_2 remains adsorbed), while there is 77% conversion for reaction with O_2. There would be much larger weight increases were gallium hydroxide or a hydrated oxide generated. However, reactions [3]–[5] and [6]–[8] probably all take place when both an oxidizer and a proton source are readily available, as simulated in run d of Fig. 8, where an ethane/O_2 mixture was adsorbed, and in run e, where the O_2 was water-saturated. The weight gains here exceed (by 18% for run e and slightly less for d) the expected weight gains based on just the stoichiometry of reactions (6) or (7), and are therefore consistent with gains based on reactions [3]–[5] and [8], and also with the FTIR data.

Further evidence that H_2O adsorption at high temperature can be specific, i.e., associated with the formation of specific hydrated cations, is provided by the results of run b in Fig. 8. We found previously that the stepwise thermal desorption in He of a strong base such as 1-PA leaves a residue of heavy olefinic material (about 10% by weight of the original 1-PA) which remains associated with Ga cations (30). In Fig. 8 we see that this residue greatly reduces the amount of water adsorbed.

The pyridine absorbances on the catalysts are shown in Table 2, using the bands at 1542 and 1455 cm^{-1} (for Brønsted and Lewis acid sites in MFI, respectively (31, 32). Reduction of the dried catalyst significantly decreased the measured Brønsted and increased Lewis acidity. This is consistent with replacement of protons by Ga^+, because absorption of pyridine bound to Ga ions is also near 1455 cm^{-1} (10). Oxidation then restored some Brønsted acidity while greatly decreasing this Lewis acidity. Re-reduction of the oxidized material had the opposite effect; however, it did not fully restore the Lewis acidity, possibly because after all these treatments dealumination and structural degradation was a factor. Water treatment of the reduced material increased Brønsted acidity to close to that of the oxidized sample. These trends are in agreement with the above IR and TGA results.

The adsorption of 1-PA (50 Torr) at 323 K takes place on both Ga cations and Brønsted sites, as evidenced by the decrease in the intensity of the 3660 and 3740 cm^{-1} bands, with strong absorption at lower frequencies. The new bands (after purging with He) corresponded closely to bands previously observed upon 1-PA adsorption on H-MFI or NaH-Y (32–33), or for liquid 1-PA. At 323 K, similar bands were obtained on H-MFI, Ga_2O_3/MFI-i, and Ga-MFI-i. However, the spectrum of Ga-MFI-i differed markedly from the others when the temperature was raised to 593 K, or if 1-PA was adsorbed at 593 K. The low temperature bands were greatly attenuated. New bands appeared at 3240–3260 (ν_{N-H}), 1590 ($\delta_{N-H,asymm.}$) and especially at 1500 ($\delta_{N-H,symm.}$). These represent shifts to lower frequencies of 20–30 cm^{-1} from comparable bands of adsorbed 1-PA.

For H-MFI, 593 K is in the "plateau" region where a 1:1 complex between Brønsted acid centers and certain amines remains after adsorption at r.t. followed by heating (32, 34). At higher temperatures the complex decomposes by a reaction akin to Hofmann elimination to form NH_3 and alkenes, here propene. But we have shown that for Ga-MFI materials with Ga:Al = 1:1 such complexes are not formed exclusively (2). Rather, NH_3 can be desorbed at below 600 K because a transalkylation reaction may take place (2, 30),

TABLE 2

Absorbances of Pyridine (423 K) on Ga-MFI Catalysts, Various Pretreatments

Sample	At 1542 cm^{-1}	At 1455 cm^{-1}
Unreduced (Ga_2O_3/MFI-i)	0.43	0.18
Reduced[a]	0.20	0.51
Reduced/oxidized[b]	0.24	0.29
Reduced/oxidized/reduced	0.19	0.31
Reduced/H_2O[c]	0.25	0.19

[a] Using 25% H_2/He at 823 K, 3 h.
[b] Oxidized with 25% O_2/He at 823 K, 1 h.
[c] Exposed to water-saturated (at r.t.) He for 15 min at 823 K.

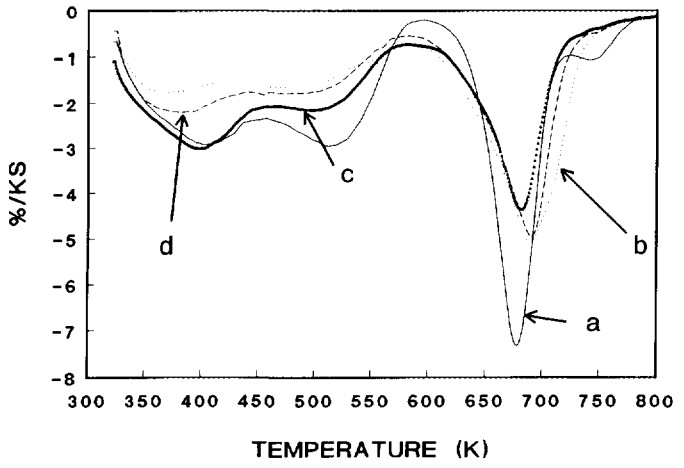

FIG. 9. Thermal analysis (DTA curves) of 1-PA for: (a) H-MFI, dried at 773 K; (b) Ga-MFI-i; (c) Ga-MFI-i treated with H_2O-saturated He at 823 K; (d) same as (c), but then reduced again at standard conditions.

$$[(C_3H_7NH_3)_2Ga]^+Z^- \rightarrow NH_3 + [(C_3H_7)_2NHGa]^+Z^-. \quad [9]$$

The existence of the dipropylamine (DPA) complex was suggested based on TGA measurements and analysis of the products of decomposition of this complex, including nitriles and imines.

The band shifts we observed for Ga-MFI-i at 593 K are consistent with production of an adsorbed DPA complex, as DPA is a stronger base than 1-PA. As a check, we examined liquid DPA by FTIR and found strong absorption in the 3250–3400 cm^{-1} and 1500 regions and moderate absorption at 1580–1590. Therefore transalkylation of 1-PA is characteristic of reduced Ga-MFI materials, and there is good correspondence between the FTIR and TGA studies of 1-PA adsorption and reaction.

These results can be put to good use in interpreting the changes associated with O_2 and H_2O adsorption onto catalysts such as Ga-MFI. Figure 9 gives microbalance DTGA data for the desorption in He of 1-PA from H-MFI, reduced Ga-MFI-i, and reduced, water-treated Ga-MFI-i. The first two are the same as in past work (2, 30) and show that reducing Ga_2O_3/MFI decreases the two low-temperature DTA features (associated with the formation of 3:1 and 2:1 1-PA/framework Al complexes, respectively), while shifting and broadening the main DTA feature centered at 678 K for H-MFI and 689 K for Ga-MFI. The differences at the lower temperatures are due to the aforementioned DPA complex, while the difference in the higher temperature feature results from lower temperature desorption of NH_3 along with the formation of imines and nitriles, which desorb at higher temperatures (2, 30). The disappearance of the peak associated with strongly acidic sites in H-MFI (at 747 K) was also shown to be characteristic of reduced Ga materials.

In Fig. 9 we see that, after the adsorption of water, the 1-PA desorption spectrum is qualitatively similar to that of H-MFI, while a second reduction changes it back in the direction of reduced Ga-MFI-i. Note the change in the main desorption feature (at 689 K for Ga-MFI-i and 691 K for reduced/water treated/reduced Ga-MFI-i). Only the very high temperature H-MFI feature fails to reappear on water treatment, which might be expected as it is usually associated with Lewis sites on H-MFI, which might not be present after water treatment. Finally, treatment with both O_2 and H_2O simultaneously (as in run e, Fig. 8) gave a DTA spectrum the same as that obtained upon treatment with H_2O alone.

The quantitative DTA results reinforce the conclusion that proton sites can be regenerated through both oxidation and hydrolysis, and then removed again by reduction. The moles of 1-PA adsorbed per Al atom at the beginning of the primary desorption feature were 1.0 for H-MFI, 1.7 for Ga-MFI-i (corresponding almost exactly to a 1:1 DPA/Ga^+ complex), 0.97 for the material treated with O_2 and H_2O, 0.89 for the water-treated material, and 1.2 for the water-treated/rereduced material. So the amount of adsorbed amine did decrease and then increase as water was adsorbed and then desorbed. However, the amounts of equivalent adsorbed 1-PA molecules per Al in the re-reduced material was still less than 1.7, probably because all of the water could not be displaced from Ga cations, in agreement with the IR results (Fig. 7). There is also the possibility that some dealumination took place during the slow thermal analysis.

The DTGA curves for O_2-treated materials are shown in Fig. 10. Note that it is impossible to exclude H_2O during 1-PA thermal analysis when O_2 is present, because dehydrogenation to nitriles begins at temperatures as low as

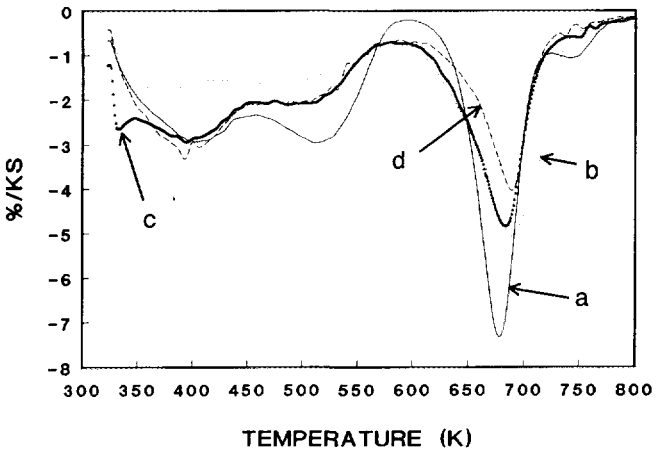

FIG. 10. Thermal analysis (DTA curves) of 1-PA for: (a) H-MFI, dried at 773 K; (b) Ga-MFI-i; (c) Ga-MFI-i treated with 30% O_2/70% He at 823 K; (d) Ga-MFI-i treated with 12% ethane/2% O_2/86% He at 823 K.

530 K for Ga-MFI (30). Therefore we expect the primary desorption feature for reoxidized Ga-MFI-i (at 683 K vs 678 K for H-MFI, 689 K for Ga-MFI-i, and 689 K for C_2H_6/O_2-treated Ga-MFI-i) to resemble that of H-MFI. Aside from the shift to lower temperature and the narrowing of this feature (typical of the simultaneous desorption of propene and NH_3 which occurs in H-MFI), there were also increases in the magnitudes of the first two desorption features. The reoxidized Ga-MFI-i adsorbed only 1.1 mol 1-PA per Al. The material treated with the higher partial pressure of O_2 showed the greater shift toward H-MFI behavior.

DISCUSSION

The conversion of the lower alkanes and alkenes to aromatics involves alkane dehydrogenation and alkene oligomerization and cyclization. The Ga-MFI catalysts are conventionally thought of as bifunctional; Ga accelerates the dehydrogenation process, by increasing the rate of H_2 recombinative desorption (35, 36), while oligomerization and cyclization of olefins is thought to occur on the Brønsted acid sites of the zeolites (37). However, high surface area Ga_2O_3 and steamed gallosilicates (with little measurable Brønsted acidity) by themselves can aromatize dienes, 1-hexene, and cyclohexene at significant rates over the range 770–870 K (38, 39). For alkanes C_3 and larger, the formation of aromatics, while sensitive to H_2 partial pressures (as in Table 1) (40), is less sensitive to the almost complete absence of protons (4, 6, 7). Zeolitic Ga cations, with enhanced Lewis acid strengths resulting from the electron-withdrawing nature of the zeolite, may catalyze almost the entire transformation without the intervention of zeolite proton sites. The strong Lewis acidity associated with reduced Ga cations at lattice sites has been measured through changes in EPR intensity upon adsorption of electron donors (22), in the IR frequency of pyridine (41) or CO adsorption (35), and in NH_3 TPD (13). The thermal analysis data for 1-PA presented here also indicate the presence of strongly acidic sites in reduced Ga-MFI, even when the FTIR data indicate almost no zeolite proton sites are present.

The Ga-MFI was activated by reduction with H_2. Price and Kanazirev have suggested, based on TGA data for mixtures similar to Ga_2O_3/MFI-m, that Ga_2O_3 is dispersed in the zeolite as follows (4):

$$Ga_2O_3 + 2\,H_2 \rightarrow Ga_2O + 2\,H_2O \qquad [10]$$

$$Ga_2O + 2\,H^+Z^- \rightarrow H_2O + 2\,Ga^+Z^-. \qquad [11]$$

This dispersion by reduction has been confirmed through a variety of FTIR (23), STEM (42), EXAFS (36), and XPS (6, 43) studies, and the mechanical mixture used here (Ga_2O_3/MFI-m) was reduced quantitatively in agreement with the above stoichiometry. Reduced catalysts are more active for alkane dehydrogenation than unreduced Ga_2O_3/H-MFI mixtures (3, 4, 10); results suggesting the contrary were obtained either at high conversions (44), and so may be attributed to rapid *in situ* dispersion, or at higher temperatures and Ga/Al ratios well below one (12, 45). Even in this latter case, the dispersion of Ga caused by contacting Ga_2O_3 and H-MFI under reaction conditions resulted in increases in aromatics selectivity with time on stream (45), behavior not observed with H-MFI (46).

After dispersion, some of the Ga^+ in the zeolite can revert to a higher formal oxidation state (9, 13, 36), which as seen here is the preferred equilibrium state at temperature <700 K. Based on current FTIR and thermal analysis results and our previous work, we can conclude that the redox pretreatments used here converted some Ga^+ back to $[GaO_x]^{3-2x}$, where $x \sim 1$. The reaction of Ga^+ with H_2O does not proceed exactly as the reverse of reactions [10] and [11], because there is no evidence that liberated Ga_2O exits the zeolite. Were this the case, the facile redox behavior shown in Figs. 6 and 7 would be impossible, as it takes about 2 ks to initially reduce a small Ga_2O_3/MFI-i sample in a microbalance pan, while the re-reduction observed in the FTIR cell is rapid. Therefore reactions [4] and [5] and [7] and [8] are the most likely result when H_2O is contacted with reduced Ga/MFI, while reactions [3] and [6] take place as well when both O_2 and H_2O are present.

This chemistry helps explain the behavior found in ethane dehydrogenation, with the overriding assumptions that this reaction is critically dependent on a balance between proton and Ga cations, which are mostly in the reduced state under reaction conditions (36). The dynamic nature of the redox process makes it impossible to estimate the exact percentage of total exchange sites which should be Ga^+ for optimal activity. But we can say that the number of proton sites generated by the admission of a small amount of O_2 to the feed (Fig. 3), or by a pretreatment with dry O_2 (Figs. 1 and 2), was sufficient to initially boost overall catalyst activity and the yield to aromatics. However, the larger number of proton sites generated by reaction with H_2O immediately destroyed dehydrogenation activity (Fig. 3), which can be restored when H_2O is removed (Fig. 4) because of the proximity of intrazeolitic gallium oxide and the presence of H_2. Water also inhibits the adsorption and desorption of H_2, and promotes the adsorption of O_2, even on pure gallium oxides (46); this might tend to further reduce the overall catalytic activity. These results suggest that the optimal fraction of exchanged Ga cations is near, but not equal to, 100%.

These results are consistent with a hypothesis that a few zeolite proton sites, in conjunction with nearby Ga^+ sites, are needed to generate carbenium ion chain carriers (CH_3 CH_2^+), which then rapidly undergo dehydrogenation, oligo-

merization, and dehydrocyclization (48, 49). The catalytic cycle can be perpetuated by an H-transfer reaction of arenium, benzylic, or a similar carbenium ion with ethane. This view avoids the necessity of postulating an exclusively Ga^+- or Ga_2O_3-mediated ethane activation step, which ascribes to them superacid properties.

The concept of an optimum number of proton sites is consistent with other careful studies of initial activity and aromatics yield in propane aromatization (13), although the mechanism proposed here is slightly different. In particular, we have shown that excess formation of specifically $[GaO]^+$ or $[Ga(OH)_2]^+$ is detrimental to both overall catalytic activity and aromatics formation, even though these should be stronger Lewis acids than Ga^+.

However, the promotion by CH_4 of C_2H_6 dehydrogenation (Fig. 5) does not fall neatly into this scheme and is seemingly incompatible with results from C_3H_8/CD_4 cross-exchange studies (16). In these experiments, CH_4 reacted on Ga-MFI, presumably to hydrogen-deficient surface carbon and H_2. This reaction was evident as well in our past work (19); catalysts contacted with just CH_4 accumulated weight at temperatures typical of ethane dehydrogenation. The TPO results in Table 1 confirm that the presence of CH_4 triggered extra weight accumulation. The extra H_2 produced by the reaction of CH_4 might therefore be expected to inhibit the normal reactions of C_2H_6, even though gaseous hydrocarbon products are not obtained with pure CH_4 feeds at these temperatures (19). This was indeed the case for longer times on stream.

We also found no evidence that CH_4 by itself would alter the chemistry at the Ga cation sites. After adsorption at 823 K on Ga-MFI-i, the equivalent of 0.30 mol CH_4/mol Al was present on the catalyst, and we observed a DTGA spectrum for 1-PA thermal analysis qualitatively similar to that of Ga-MFI-i. Prior to the primary desorption feature there remained the equivalent of ~1 mol adsorbed/mol Ga (0.75 mol DPA complex plus 0.30 mol CH_4), as compared to ~1.0 mol DPA complex for Ga-MFI-i.

Therefore the behavior observed in Fig. 5 at short times on stream must have a different explanation. It is possible that hydrogen-deficient CH_x on the catalyst may promote formation of aromatics by mediating H-transfer from ethane to larger carbenium ions. This hypothesis is supported by ethane-only reaction results. It is seen (Table 1) that the catalyst is more active for aromatics formation after two cycles of reduction/reaction. This was found to be true even when the initial reduction period was doubled in order to ensure reduction of Ga_2O_3—without effect on the initial yield. We hypothesize that the second reduction, that of the used catalyst, generated CH_4 from the coke, and therefore was similar to treatment with CH_4 itself. The CH_x deposited from CH_4 should be different from carbon deposited through heavier alkene and PAH formation ("coke"), and it must be this carbon which promotes the ethane dehydrogenation at short times.

CONCLUSIONS

1. Addition of small amounts of water and/or O_2 to reduced Ga-MFI catalysts during the reaction of ethane has the primary effect of increasing the number of zeolite proton sites and reoxidizing Ga cations to dispersed Ga oxide.
2. The dehydrogenation of ethane to aromatics is optimal when the fraction of exchange sites in the zeolite which are protons is small. There must be exchanged Ga^+ in the working catalyst, not just nearby Ga oxide.
3. An increase in zeolite proton sites above low levels immediately decreases both selectivity to aromatics and activity. The process is reversible within limits.
4. Preadsorption or cofeeding of methane with ethane also increases the production of aromatics, at least at short times on stream. This phenomenon appears to arise from the action of adsorbed $(CH)_x$ fragments.

ACKNOWLEDGMENTS

We gratefully acknowledge the financial support of the Department of Energy (Grant DE-FG05-92ER14291) and the Exxon Education Foundation. We thank Vaughan Hart for experimental assistance.

REFERENCES

1. Guisnet, M., Gnep, N. S., and Alario, F., *Appl. Catal. A* **89,** 1 (1992).
2. Kanazirev, V., Dooley, K. M., and Price, G. L., *J. Catal.* **146,** 228 (1994).
3. Kanazirev, V., Price, G. L., and Dooley, K. M., *J. Chem. Soc. Chem. Commun.* **9,** 712 (1990).
4. Price, G. L., and Kanazirev, V., *J. Catal.* **126,** 267 (1990).
5. Price, G. L., and Kanazirev, V., *J. Mol. Catal.* **66,** 115 (1991).
6. Kanazirev, V., Price, G. L., and Dooley, K. M., *in* "Zeolite Chemistry and Catalysis" (P. A. Jacobs *et al.*, Eds.), p. 277. Elsevier, Amsterdam, 1991.
7. Kanazirev, V., Dimitrova, R., Price, G. L., Khodakov, A. Yu., Kustov, L. M., and Kazansky, V. B., *J. Mol. Catal.* **70,** 111 (1991).
8. Price, G. L., Kanazirev, V., and Dooley, K. M., U.S. Patent 5,449,579 (1992).
9. Dooley, K. M., Chang, C., and Price, G. L., *Appl. Catal. A* **84,** 17 (1992).
10. Meriadeau, P., Abdul-Hamid, S. B., and Naccache, C., *J. Catal.* **139,** 679 (1993).
11. Jia, S., Wu, S., and Meng, Z., *Appl. Catal. A* **103,** 259 (1993).
12. Buckles, G., and Hutchings, G. J., *Catal. Lett.* **27,** 361 (1994).
13. Kwak, B. S., and Sachtler, W. M. H., *J. Catal.* **145,** 456 (1994).
14. Fujimoto, K., Nakamura, I., and Yokota, K., *Zeolites* **9,** 120 (1989).
15. Xu, W.-Q., and Suib, S. L., *J. Catal.* **145,** 65 (1994).
16. Iglesia, E., and Baumgartner, J. E., *Prepr. ACS Div. Petrol. Chem.* **38,** 746 (1993).
17. Li, Y., and Armor, J. N., *J. Catal.* **145,** 1 (1994).
18. von Ballmoos, R., "Collection of Simulated XRD Powder Patterns for Zeolites." Butterworths, Boston, 1984.
19. Samarth, R. D., and Dooley, K. M., *Appl. Catal. B* **5,** 71 (1994).
20. Parker, L. M., Bibby, D. M., and Burns, G. R., *Zeolites* **13,** 107 (1993).

21. Simmons, D. K., Szostak, R., Agrawal, P. K., and Thomas, T. L., *J. Catal.* **106,** 287 (1987).
22. Khodakov, A. Yu., Kustov, L. M., Bondarenko, T. N., Dergachev, A. A., Kazansky, V. B., Minachev, Kh. M., Borberly, G., and Beyer, H. K., *Zeolites* **10,** 603 (1990).
23. Meriadeau, P., and Naccache, C., *Appl. Catal. A* **73,** L13 (1991).
24. Meriadeau, P., and Primet, M., *J. Mol. Catal.* **61,** 227 (1990).
25. Kubelkova, L., Beran, S., and Lercher, J. A., *Zeolites* **9,** 539 (1989).
26. Zholobenko, V. L., Kustov, L. M., Borovkov, V. Yu., and Kazansky, V., *Zeolites* **8,** 175 (1988).
27. Maijanen, A., Derouane, E. G., and Nagy, J. B., *Appl. Surf. Sci.* **75,** 204 (1994).
28. Zholobenko, V. L., Kustov, L. M., Kazansky, V. B., Loeffler, E., Lohser, U., Peuker, Ch., and Oehlmann, G., *Zeolites* **10,** 304 (1990).
29. Zundel, G., "Hydration and Intermolecular Interaction," Chap. 2. Academic Press, New York, 1969.
30. Kanazirev, V. I., Price, G. L., and Dooley, K. M., *J. Catal.* **148,** 164 (1994).
31. Topsoe, N.-Y., Pedersen, K., and Derouane, E. G., *J. Catal.* **70,** 41 (1981).
32. Parrillo, D. J., Adamo, A. T., Kokotailo, G. T., and Gorte, R. J., *Appl. Catal.* **67,** 107 (1990).
33. Jacobs, P. A., and Uytterhoeven, J. B., *J. Catal.* **26,** 175 (1992).
34. Gricus Kofke, T. J., Gorte, R. J., and Kokotailo, G. T., *Appl. Catal.* **54,** 177 (1989).
35. Iglesia, E., Baumgartner, J. E., and Price, G. L., *J. Catal.* **134,** 549 (1992).
36. Meitzner, G. D., Iglesia, E., Baumgartner, J. E., and Huang, E. S., *J. Catal.* **140,** 209 (1993).
37. Gnep, N. S., Doyemet, J. Y., and Guisnet, M., *in* "Zeolites as Catalysts, Sorbents and Detergent Builders" (H. G. Karge and J. Weitkamp, Eds.), p. 153. Elsevier, Amsterdam, 1989.
38. Meriadeau, P., Sapaly, G., and Naccache, C., *in* "Chemistry of Microporous Materials" (T. Inui, S., Namba, and T. Tatsumi, Eds.), p. 267. Elsevier, Amsterdam, 1991.
39. Bayense, C. R., van der Pol, A. J. H. P., and van Hooff, J. H. C., *Appl. Catal.* **72,** 81 (1991).
40. Merideau, P., and Naccache, C., *in* "Zeolite Chemistry and Catalysis" (P. A. Jacobs, N. I. Jaeger, L. Kubelkova, and B. Wichterlova, Eds.), p. 405. Elsevier, Amsterdam, 1991.
41. Roessner, F., Hagen, A., Mroczek, U., Karge, H.-G., and Steinberg, K.-H., *in* "Proceedings, 10th International Congress on Catalysis, Budapest, 1992" (L. Guczi, F. Solymosi, and P. Tetenyi, Eds.), Vol. B, p. 1707. Elsevier, Amsterdam, 1993.
42. Joly, J. F., Ajot, H., Merlen, E., Raatz, F., and Alario, , *Appl. Catal. A*, **79,** 249 (1991).
43. Carli, R., Bianchi, C. L., Giannantonio, R., and Ragaini, V., *J. Mol. Catal.* **83,** 379 (1993).
44. Le Van Mao, R., Yao, J., and Sjiariel, B., *Catal. Lett.* **6,** 23 (1990).
45. Buckles, G. J., and Hutchings, G. J., *J. Catal.* **151,** 33 (1995).
46. Bayense, C. R., and van Hooff, J. H. C., *Appl. Catal. A* **79,** 127 (1991).
47. Reti, F., Fleischer, M., Meixner, H., and Giber, J., *Sensors Actuators B* **18,** 138 (1994).
48. Derouane, E. G., Abdul Hamid, S. B., Ivanova, I. I., Blom, N., and Hojlund-Nielsen, P.-E., *J. Mol. Catal.* **86,** 371 (1994).
49. Kwak, B. S., Sachtler, W. M. H., and Haag, W. O., *J. Catal.* **149,** 465 (1994).